International Journal of Mass Spectrometry 286 (2009) 70–82

Contents lists available at ScienceDirect

International Journal of Mass Spectrometry

journal homepage: www.elsevier.com/locate/ijms

Isotope ratio analysis of actinides, fission products, and geolocators by high-efficiency multi-collector thermal ionization mass spectrometry

S. Bürger*, L.R. Riciputi**, D.A. Bostick, S. Turgeon[1], E.H. McBay, M. Lavelle

Chemical & Isotope Mass Spectrometry Group, Transuranium Research Institute, Chemical Sciences Division, Oak Ridge National Laboratory, P.O. Box 2008, Oak Ridge, TN 37831-6375, USA

ARTICLE INFO

Article history:
Received 14 May 2009
Received in revised form 19 June 2009
Accepted 19 June 2009
Available online 27 June 2009

Keywords:
Multi-collector thermal ionization mass spectrometry
Multiple-ion counting
Efficiency
Detection limit
Isotope ratio analysis

ABSTRACT

A ThermoFisher "Triton" multi-collector thermal ionization mass spectrometer (MC-TIMS) was evaluated for trace and ultra-trace level isotope ratio analysis of actinides (uranium, plutonium, and americium), fission products and geolocators (strontium, cesium, and neodymium). Total efficiencies (atoms loaded to ions detected) of up to 0.5–2% for U, Pu, and Am, and 1–30% for Sr, Cs, and Nd can be reported employing resin bead load techniques onto flat ribbon Re filaments or resin beads loaded into a millimeter-sized cavity drilled into a Re rod. This results in detection limits of <0.1 fg (10^4 atoms to 10^5 atoms) for $^{239-242+244}$Pu, $^{233+236}$U, $^{241-243}$Am, ^{89,90}Sr, and ^{134,135,137}Cs, and ≤1 pg for natural Nd isotopes (limited by the chemical processing blank) using a secondary electron multiplier (SEM) or multiple-ion counters (MICs). Relative standard deviations (RSD) as small as 0.1% and abundance sensitivities of 1×10^6 or better using a SEM are reported here. Precisions of RSD ≈0.01–0.001% using a multi-collector Faraday cup array can be achieved at sub-nanogram concentrations for strontium and neodymium and are suitable to gain crucial geolocation information. The analytical protocols reported herein are of particular value for nuclear forensic and nuclear safeguard applications.

1. Introduction

Various analytical methods have been developed and are being utilized by laboratories around the world to meet the challenge of providing increasingly sensitive, precise, and accurate information in actinide and fission product research. This includes questions posed by nuclear forensic investigations and the attribution of illegally trafficked nuclear material ("nuclear smuggling") and nuclear safeguards [1–5], bioassay [6–11], environmental monitoring [11–19] and post-detonation attribution and nuclear accident analysis [20–27]. These analytical methods are also applied for speciation of actinides and assessment of contaminated sites and nuclear waste repositories [28–35], studies of geological and biological cycles [36–39], search for transuranics and extinct or primordial radionuclides in nature [40–46], burn-up and post-irradiation examination of nuclear fuels [47–52], reactor fuel performance [53,54], as well as determination of half-lives [55–57] and ionization potentials [58–62], metrology [63–65], and nuclear structure research [66,67].

In the nuclear forensic context, isotopic composition [1,2,4,68–77] is of primary concern, in addition to the determination of physical parameters (including roughness, microstructure, geometry) [2–4,78–80], chemical structure (e.g., mineralogical structure, metallurgical information, oxidation states) [81–83], impurity and analyte content [2,3,77,78,84–87], geolocation signatures (e.g., host rock, climate) [3,88–91], or age since last chemical treatment [3,90,92–96]. Isotope ratio analysis can be particularly useful in revealing the origin and history of nuclear materials. As can be seen in Table 1, the knowledge of the isotopic composition of uranium or plutonium can provide information about the source of the material. Additionally, the isotopic composition of elements like strontium, neodymium, lead, and stable isotopes (H, C, N, O, and S) encodes details about the geographic provenance and potentially the geographic origin; it is being utilized in a variety of scientific fields including forensic investigations [88,91,97–103]. Isotope ratio analysis of various fission products can, for example, provide useful information on the burn-up of nuclear fuels [3,47,48]. Isotope dilution techniques (spiking) permit highly accurate determination of elemental concentrations [104–106] and radioactive tracers can be used, for example, to

* Corresponding author. Present address: Department of Energy, New Brunswick Laboratory, 9800 South Cass Avenue, Bldg 350, Argonne, IL 60439, USA. Tel.: +1 630 252 2466.
** Corresponding author. Present address: Nuclear & Radiochemistry Group, Los Alamos National Laboratory, P.O. Box 1663, Los Alamos, NM 87545, USA.
E-mail address: stefan.buerger@ch.doe.gov (S. Bürger).
[1] Present address: Dept. of Earth & Atmospheric Sciences, University of Alberta, Edmonton, AB T6G 2E3, Canada.

1387-3806/$ – see front matter © 2009 Elsevier B.V. All rights reserved.
doi:10.1016/j.ijms.2009.06.010

Table 1
Isotopic composition (in atom percent) of uranium and plutonium originating from different sources; [#]initial core enrichment; [$]uranium materials with U-235 enrichments of significantly less than 90% can be used to build fission weapons; [&]Oralloy = Oak Ridge Alloy.

Uranium source	^{233}U	^{234}U	^{235}U	^{236}U	^{238}U
Natural uranium (NU) [65,72,73,166,167]		0.0050–0.0059	0.7198–0.7207	10^{-8} to 10^{-11}	99.2739–99.2752
Depleted uranium (DU) [168]			<0.7		
Low enriched uranium (LEU) [168]			>0.7 and <20		
High enriched uranium (HEU) [168]			>20		
Weapon-grade uranium/Oralloy[&] [3]			≥ 90[$]/≈93.5		
Western type pressurized water reactor (PWR)[#] [169]			1.3–5 (9)		
Russian type pressurized water reactor (VVER)[#] [169]			1.5–4.4		
Boiling water reactor (BWR)[#] [169]			0.7–3.7		
MAGNOX[#] [169]			Natural		
Pressurized heavy water reactor (PHWR)[#] [169]			Depleted to 1.5		
Russian type light water graphite reactor (RBMK)[#] [169]			1.8–2.4		

Plutonium source	^{238}Pu	^{239}Pu	^{240}Pu	^{241}Pu	^{242}Pu
Global fallout, northern hemisphere (average) [170]		83.5	15.0	1.2	0.3
Medical grade ^{238}Pu [171]	90.4	9.0	0.6	0.3	0.1
Light water reactor (LWR)					
20 GWd/t burn-up	0.5	73.5	20.0	5.0	1.0
30 GWd/t burn-up	1	60	22	13	4
60 GWd/t burn-up [171]	4.4	46.3	24.9	12.7	11.7
MAGNOX, 5 GWd/t burn-up [171]		68.5	25.0	5.3	1.2
Chernobyl nuclear accident, 1986, environmental samples [62,172]	0.21–0.31	66.2–71.8	21.98–26.1	4.7–6.21	1.2–1.8
Weapons grade, <1 GWd/t burn-up [171]	0.04	93.3	6.0	0.6	0.04
Nagasaki, nuclear explosion, 1945 [25]		94.5	5.5		

study natural biological cycles or environmental behavior of actinides.

For ultra-low level isotope ratio analysis of stable isotopes or radionuclides with long half-lives, mass spectrometry is the most powerful analytical tool to date, as can be seen from Table 2, which compares detection limits of various analytical techniques. While extremely low detection limits are possible via ion counting for radioisotopes with comparably short half-lives, the lowest detection limits for radionuclides with comparably long half-lives however have been demonstrated using Faraday cup multi-collector sector-field mass spectrometry (see Table 2), as well as highest precisions in isotope ratio measurements [107].

Thermal ionization mass spectrometry (TIMS) [72,108–112], inductively coupled plasma mass spectrometry [113–120], secondary ion mass spectrometry (predominately for particle or surface analysis) [71,54], accelerator mass spectrometry (predominately for high abundance sensitivity analysis) [10,121–124], and resonance ionization mass spectrometry (high elemental selectivity) [19,125–128] are frequently utilized for analysis of actinides and other radionuclides. Glow discharge mass spectrometry has been used for isotope ratio analysis of actinides, such as uranium [129–131], as well as fission-track TIMS for particles [132]. Nanosecond laser ablation ICP-MS [133–137] and laser ablation isotope dilution ICP-MS [138,139] have been utilized for isotope ratio analysis of nuclear samples. New developments that are being explored for radioanalytics include laser ablation ion storage time-of-flight mass spectrometry [140,141] and femto-second laser ablation ICP-MS [142,143]. Some of the applications of mass spectrometry in nuclear research have been reviewed by DeLaeter [67] and DeLaeter and Kurz [144].

Multi-collector sector-field mass spectrometry protocols have demonstrated some of the lowest detection limits for isotope ratio analysis of actinides (see Table 2) and other stable or long-lived nuclides. Highest precisions in isotope ratio analysis are traditionally reported using MC-TIMS instruments, with relative standard deviations as low as 0.01% or better [107,186]. Various methods have been developed to enhance the total/ionization efficiency (and thus the detection limit and precision) of TIMS, e.g., using carbon additives, benzene gas, and resin bead loads [110,145–147,178], or platinum coating and electrodeposition [148]. These methods aim to reduce the formation of oxides, improve beam focus and ion transmission by reducing the spatial extent of the sample load, or enhance the work function of the ionizer materials (usually rhenium, tantalum, tungsten or platinum).

Enhanced ion beam stability and reduced isotope mass fractionation have been observed using platinum or carbon coatings [149]. Efficiency (and thus detection limit) of a TIMS system can also be improved by replacing the conventional flat ribbon filament with a cavity ion source (also know as crucible, i.e., a millimeter size cavity drilled into a rod, which is similar to electro-thermal vaporization or ETV). Higher ionization efficiencies are theoretically feasible due to the larger ratio of surface area to volume, higher operating temperatures, and confined geometry [150–154]. The actual contribution to the formation of the ions by thermal ionization (enhanced by multiple atom–wall collisions inside the cavity), electron bombardment (i.e., electron-impact), and field ionization is yet unknown. The high-temperature cavity is known to be an efficient ion source for elements with high ionization potential (below ≈7 eV; e.g., uranium, plutonium, or thorium). Previous studies on uranium and plutonium at Oak Ridge National Laboratory and the IAEA's Safeguard Analytical Laboratory, Austria, showed the possibility of high ionization efficiency when utilizing this ion source coupled to a single-collector TIMS [155,156]. We present here an evaluation of a cavity source-equipped ThermoFisher "Triton" multi-collector thermal ionization mass spectrometer for trace and ultra-trace level isotope ratio analysis of actinides (uranium, plutonium, and americium), fission products, and geolocators (strontium, cesium, and neodymium). We compare conventional filament techniques with the cavity ion source, as well as different sample loading and preparation techniques. We also assess the use of secondary electron multiplier, multiple-ion counters, and Faraday cup multi-collectors.

Table 2
Detection limits of various analytical methods used for isotope ratio analysis of actinides. Note that detection limits are reported using different confidence levels and are sometimes stated as quantification limits (see referenced papers). #Combined ^{239}Pu and ^{240}Pu signal, ratio not resolved, $239Pu and ^{240}Pu ratio resolved, &detection limits can be improved using longer counting times.

Analytical method	Nuclide	Detection limit/g	
α-Spectrometry&	^{232}Th	2.5×10^{-8}	[113]
	^{235}U; ^{238}U	1.3×10^{-9}; 8.1×10^{-9}	[113]
	$^{239+240}$Pu#	10^{-14}	[113,173]
	^{239,240}Pu$	10^{-13} to 10^{-12}	[174]
	^{242}Pu; ^{244}Pu	10^{-13}; 10^{-11}	[173]
Neutron activation analysis	^{235}U	10^{-11} to 10^{-10}	[175]
	^{238}U	10^{-11}	[176]
	^{239}Pu	10^{-13}	[177]
	^{242}Pu; ^{244}Pu	10^{-12} to 10^{-11}; 10^{-11} to 10^{-10}	[175]
AMS	^{236}U	$\approx 10^{-16}$	[122]
	$^{239,240-244}$Pu	10^{-17} to 10^{-15}	[10,121,123,124]
TIMS	U	10^{-15} to 10^{-14}	[70,148]
	$^{233+236}$U	10^{-17} to 10^{-16}	This work
	^{237}Np	$\approx 10^{-17}$	[15]
	$^{239,240-244}$Pu	10^{-17} to 10^{-15}	[8,10,15,70,110,159,178]
		10^{-17} to 10^{-16}	This work, [90]
	Am	10^{-16}	[70]
	$^{241-243}$Am	10^{-17} to 10^{-16}	This work
SIMS	U and Pu	10^{-9} to 10^{-12} g/g	[71]
ICP-QMS	^{232}Th	1×10^{-12}	[113]
	$^{234-236,238}$U	10^{-15} to 10^{-11}	[113,114]
	^{237}Np	1×10^{-11}	[113]
	^{239,240}Pu	1×10^{-11}	[113]
(MC)-SF-ICP-MS	U	10^{-17}	[115]
	^{233,236}U	10^{-17} to 10^{-16}	L.R. Riciputi (unpublished results)
	^{237}Np	7×10^{-16}	[116]
	$^{239-242,244}$Pu	10^{-17} to 10^{-15}	[115–119], L.R. Riciputi (unpublished results)
	^{241,243}Am	$\approx 6 \times 10^{-16}$	[116], L.R. Riciputi (unpublished results)
RIMS	^{235,238}U	$<10^{-12}$	[125]
	^{237}Np	1.6×10^{-13}	[179]
	$^{238-242,244}$Pu	10^{-16} to 10^{-15}	[19,127,128]

2. Experimental and operational details

2.1. Reagents

High purity nitric acid (OmniTrace Ultra, EM Science Gibbstown, NJ) and deionized water (18 MΩ cm) were used in all chemical procedures. Different carbon compounds suspended in organic solvents (trade names 'Aquadag/DAG' or 'Collodion') were used as a carbon additive to some analyte loads (as described below).

2.2. Certified reference materials

Certified reference materials NBL 126, NBL 137, and IRMM 42a were used for Pu measurements, and NIST 4332d (4223a) for Am analysis. A ^{233}U + ^{236}U double-spike solution was used for uranium experiments (^{233}U/^{236}U ≈ 0.916; verified at ORNL with a ThermoFisher 'Neptune' multi-collector (MC) sector-field (SF) ICP-MS). NIST SRM 987 was used for Sr analysis and ICP-MS/AAS mono-element standards for natural Cs. A conventional certified ICP-MS/AAS mono-element standard as well as the La Jolla Nd reference material was used for natural Nd analysis.

2.3. Bead load preparation

The analyte (U, Pu, Am, Sr, Cs, or Nd) was loaded (adsorbed) onto anion resin beads (Bio-Rad AG 1 × 8) for Pu and U, cation beads (Bio-Rad AG 50 × 8) for Sr, Cs, Pu, and Am, and cation beads (Dowex 1 × 8) for Nd and U. Resin beads were wet-sieved to produce batches of homogeneous size (less than ±30% deviation in diameter within a batch). Typically, resin beads with diameters between 50 and 100 μm were used. A few beads (in triplicates) from each batch were fully dissolved and analyzed by isotope dilution on a ThermoFisher 'Neptune' MC-SF-ICP-MS to determine the total analyte amount on the beads. The amount of analyte absorbed per bead typically varied by less than 50% (1σ standard deviation) from bead to bead within the same batch; in some cases larger bead-to-bead variations have been observed depending on the analyte concentration. To load beads onto a filament or into a cavity, usually one single bead is confined with a few microliters of H_2O for cation Bio-Rad AG 50 × 8, 0.1 M nitric acid for cation Dowex 1 × 8, or 8 M nitric acid for anion Bio-Rad AG 1 × 8 resin beads. The liquid containing the bead is deposited at the base of the cavity or into the depression of a dimpled flat ribbon filament and covered with a thin (about a few hundred micrometers to 1 mm) layer of carbon additive. The dimple is a V-shaped depression that is located at equal distances from both ends of the ribbon running from edge to edge (not end to end). The V-shaped depression is ≤2 mm deep and depresses the filament at its midpoint along a length of ≤5 mm. Samples are air-dried under a hood. The resin bead acts as a 'point' source (improving the focus), as a carbon source (improving work function and reducing the oxide formation), and as an analyte reservoir [146].

2.4. Liquid load preparation (ribbon filament)

Strontium: Flat ribbon filament loading followed standard procedure [157], i.e., 1 μL TaO activator was loaded onto a degassed, single Re filament held at a current of 0.5 A. About 1 μL of the Sr solution (diluted to the desired concentration) was loaded in 8 M HNO_3 and progressively layered onto the "tacky" TaO on the

filament. The filament current was slowly increased to 1.8 A over about 1 min, then increased to a dull red glow and held for 5–10 s.

Neodymium: Flat ribbon filament loading followed standard procedure [157], i.e., 1 μL H_3PO_4 was loaded onto a degassed, double Re filament held at a current of 0.5 A. About 1 μL of the Nd solution (diluted to the desired concentration) was loaded in 2 M nitric acid and dried at a current of 0.5 A. The filament current was slowly increased to 1.8 A over about 1 min, then further increased to a dull red glow and held for 10–20 s. Parafilm was used for Sr and Nd loads to define a small central loading space on the filament and to reduce spreading of the liquid as the current is increased.

Uranium and plutonium: About 1 μL of analyte solution (diluted to the desired concentration) was loaded in 1–8 M nitric acid onto a degassed single Re filament, air-dried, and afterwards covered with a thin layer of DAG or Collodion. Parafilm was used to define a small central loading space on the filament and to reduce spreading as the current is increased. Alternatively, the filament loading technique described in [157] for uranium can be used.

Americium and cesium: Analysis of Am or Cs liquid loads onto flat ribbon filaments were not performed.

2.5. Liquid load preparation (cavity)

For cavity liquid loads of uranium, plutonium, americium, strontium, cesium, or neodymium, about 0.5–2 μL of the analyte solution (brought up in 1–8 M nitric acid) is loaded with a micropipette tip (Eppendorf Micropipette Geloader Tips) into a Re or Ta cavity. In some studies, 1 μL suspended carbon was added. The cavity loads were air-dried before mounting onto a modified TIMS sample turret.

2.6. Multi-collector thermal ionization mass spectrometer

In this study, a ThermoFisher "Triton" multi-collector TIMS was utilized. It is equipped with nine (8 + 1) solid graphite Faraday cup detectors (low noise 10^{11} Ω resistors), one center single discrete dynode secondary electron multiplier (SEM), and seven multiple-ion counters (MICs) in a 6 + 1 configuration at the outer low Faraday cup (L4). Observed Faraday cup baseline deviations were <0.01 mV (at 4 s integration time) and SEM and MIC dark noise levels ≤0.01 cps (for the integrated mass range of a single isotope). The SEM is coupled to a retarding potential quadrupole (RPQ) lens for improved abundance sensitivity. A total of up to 21 sample filaments can be loaded onto a standard "Triton" TIMS filament turret. Re filaments were degassed under vacuum to 6 A using a filament bakeout device.

2.7. Cavity procedure

The high-efficiency cavity system used here is described elsewhere [90,155]. Briefly, it consists of three parts: (1) the metal cavity, (2) two heating filaments (typically of tungsten), and (3) an electron shield. Re, W or Ta rods with a narrow cavity (approx. 0.5 mm diameter × 10 mm depth) bored into the end of a rod of ca. 1.5 mm diameter are used (further referred to as the cavity). A total of up to 21 cavities can be loaded into the TIMS on one modified sample wheel. A voltage difference of −1500 V is applied between the cavity and an electron shield, ensuring that electrons emanating from the heating filaments are focused towards the cavity and the positive ions (from the analyte) towards the electron shield. The cavity is heated via electron bombardment (2000–3000 °C). The electrons are emitted from the tungsten filaments by applying a current of up to 4.25 A. The sample inside the cavity subsequently evaporates and ionizes, and the ions are introduced into the mass spectrometer flight tube by the decreasing source lens potentials and the nominal accelerator voltage of 10 kV. The individual contribution of thermal ionization (enhanced by multiple wall collisions inside the cavity), electron bombardment (from the tungsten filaments), and field ionization to the formation of the analyte ions is currently unknown. The high-efficiency cavity source is completely interchangeable with the normal filament source within less than 15 min.

2.8. Filament procedure

Single (dimpled) flat ribbon rhenium or tantalum filaments are heated to the desired temperature by increasing the filament current by typically 50–200 mA/min. Double Re flat ribbon filament analyses of Nd were performed with a constant ionizer current of 4.5 A. When using Faraday cups, a baseline and amplifier gain calibration is performed on a daily basis; during SEM or MIC use a dark noise calibration is performed at least weekly. A source lens focus and peak center is conducted and optimized for every sample at different ion beam currents before data acquisition. The source vacuum is usually 10^{-7} mbar or better.

2.9. Measurement procedure

For strontium, the following Faraday cup configuration was used: L2 = ^{84}Sr, L1 = ^{85}Rb, C = ^{86}Sr, H1 = ^{87}Sr + ^{87}Rb, H2 = ^{88}Sr. No zoom optics was applied. All samples, sample processing blanks, and standards were analyzed at beam intensities typically between 0.5 and 30 V at mass ^{88}Sr, depending on load size and desired precision. Typically at least 3 runs (4 s with 50 cycles) in static mode were acquired, with each run at different (but constant) beam intensity.

For neodymium, the following Faraday cup configuration was used: L3 = ^{140}Ce, L2 = ^{142}Nd, L1 = ^{143}Nd, C = ^{144}Nd, H1 = ^{146}Nd, H2 = ^{147}Sm, H3 = ^{148}Nd, H4 = ^{150}Nd. No zoom optics was applied. All samples, sample processing blanks, and standards were analyzed at beam intensities typically between 0.3 and 20 V at ^{144}Nd mass. Typically at least 3 runs (4 s with 50 cycles) in static mode were acquired, with each run at different (but constant) beam intensity.

For uranium and plutonium isotope ratio analyses, the secondary electron multiplier (SEM) using peak jumping mode or the multiple-ion counters in static mode were used. Using the SEM, the beam is leveled to a stable beam intensity of typically ≤10^5 cps. Then a peak jumping (magnet switching) with a 2 s acquisition time for each isotope is performed. The peak jumping is repeated until a required number of acquisitions are achieved or until the sample is totally evaporated. No results for isotope ratio measurements are presented for cesium and americium due to non-availability of Cs and Am isotope reference materials. However, for low-level Cs and Am analysis the same procedure as used for uranium and plutonium can potentially be utilized.

2.10. Data evaluation

For strontium isotope ratio analysis using multiple Faraday cups, a value of ^{86}Sr/^{88}Sr = 0.1194 (atom ratio) was used for internal mass fractionation correction, and Rb-87/Rb-85 = 0.3860 (atom ratio) to correct for Rb-87 interferences. An average ^{87}Sr/^{86}Sr atom ratio of 0.71028 ± 0.00006 (1σ, $n > 50$) for NBS 987 was found over a period of more than 18 months and multiple operators, an average ^{84}Sr/^{86}Sr atom ratio of 0.05649 ± 0.00005 (1σ, $n > 50$). The NIST certified values are 0.71034 ± 0.00026 and 0.05655 ± 0.00014 (atom ratio), respectively.

For neodymium isotope ratio analysis using multiple Faraday cups, a value of ^{146}Nd/^{144}Nd = 0.7219 was used as fractionation correction, and ^{147}Sm/^{144}Sm = 4.8387, ^{147}Sm/^{148}Sm = 1.3274, and ^{147}Sm/^{150}Sm = 2.0270 to correct for Sm interferences. ^{140}Ce was monitored but no interference correction is necessary for the radiogenic ^{143}Nd/^{144}Nd atom ratio of interest. An average

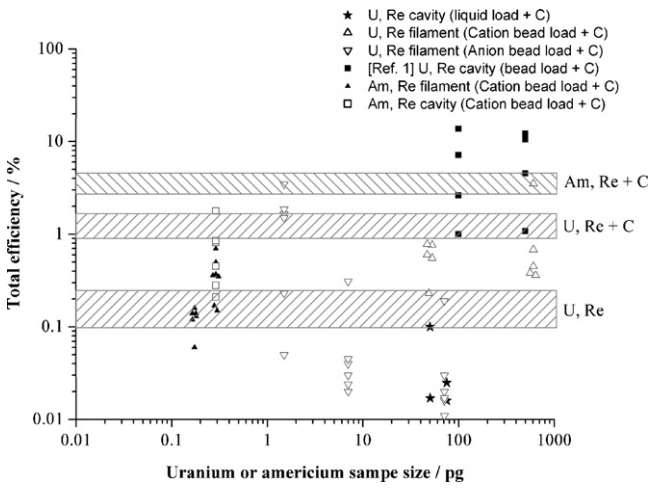

Fig. 1. Total efficiency (atoms loaded to ions detected) for uranium and americium as a function of analyte sample size using different loading techniques. Shaded areas indicate ionization efficiencies as predicated by the Saha–Langmuir equation. The predicted efficiency for Am on Re without carbon lies between U, Re and U, Re + C. [Ref. 1] refers to [155].

$^{143}Nd/^{144}Nd$ atom ratio of 0.511862 ± 0.000017 (1σ, $n > 50$) for the La Jolla standard was found over a period of more than 18 months and multiple operators, an average $^{148}Nd/^{144}Nd$ atom ratio of 0.241570 ± 0.000015 (1σ, $n > 50$). The "consensus" value is $^{143}Nd/^{144}Nd = 0.511850$ (atom ratio) [157].

For uranium and plutonium isotope ratio analysis using secondary electron multiplier or multiple-ion counters, no mass fractionation correction was applied: the observed mass fractionation of these elements using the "Triton" TIMS is small compared to the precision of the isotope ratio results when using SEM or MIC (which is limited by the ion counting statistics for low level analysis). The uncertainty stemming from the yield calibration for the SEM and calibration of the relative MICs yields are of the order of 0.1%. This too applies to the relative yields between SEM and Faraday cups.

2.11. General remarks

All experiments were performed at room temperature and atmospheric pressure. Sample preparations were performed in a class 100 clean room with a class 10 hood when necessary.

3. Results and discussion

Total efficiencies (atoms loaded to ions detected), precision, accuracy, abundance sensitivity, and detection limits were investigated for elements uranium, plutonium, americium, strontium, cesium, and neodymium.

Additionally, the measured total efficiencies are compared to the surface ionization efficiencies of the elements as predicted by the Saha–Langmuir equation in thermal equilibrium and absence of an external field (diagonally shaded areas indicated in Figs. 1, 2, 6 and 7) for Re surface or Re with a carbon layer (Re + C). Note that the measured total efficiencies reported here include the ion transmission of the sector-field mass spectrometer and detector yield. Additionally, the Saha–Langmuir equation applies only to an atomic beam impinging on a hot surface, and thus not strictly to a single filament structure, which suffers from losses of neutral analyte species due to evaporation [149]. Thus the calculated surface ionization efficiencies using the Saha–Langmuir equation can only serve as an order-of-magnitude prediction for the total efficiency to be expected. A work function of 4.96–4.98 eV for polycrystalline Re [154,158] and 5.36 eV for Re + C [154,147] was used in the calculations. Unity for the statistical weight ratio of ionic to atomic states was used, which is a good approximation for electronically complex elements [149] (like uranium, plutonium, and americium). Although for alkali elements (like cesium) it is often 1/2 [149], an approximation using unity is sufficient for assessing order-of-magnitudes (see limitations discussed above). It is assumed that the increase in the Re work function due to adding of carbon is independent of the analyte element, which might not strictly be the case.

Ta cavities were examined as an alternative surface material to Re, but the observed efficiencies using Ta cavities are a factor of 10–100 lower than those observed for Re. This is probably due to the lower work function of Ta (4.25 eV) [158]. Tungsten and graphite materials were not examined in this work. Platinum has a relative high work function (5.65 eV), but low melting point (1770 °C) [158] and a high material cost; it was not utilized as surface material in this work.

All measurements were performed in low mass resolution mode ($R_{10\%}$ about 400–500 for actinides) and (relative) standard deviations are given as 1σ unless otherwise stated.

3.1. Uranium

For uranium (see Fig. 1), a median total efficiency of 0.021% ($n = 4$) for 50–75 pg uranium liquid loads into Re cavities with carbon additive was observed. And a median total efficiency of 0.27% ($n = 28$) for 7–605 pg uranium resin bead loads (0.58% for cation beads and 0.043% for anion beads) onto dimpled flat ribbon single Re + C filaments can be reported. Loading uranium on resin beads onto filaments is about one to two orders of magnitude more efficient than loading of uranium as liquid loads onto filaments (see Table 3). It appears that there is a possible trend towards increasing efficiency with decreasing sample size, with a similar trend observed for plutonium (see below). But this needs to be examined in more detail in the future.

Resin bead loads into Re cavities were also studied, but provide significantly lower efficiencies. This is mainly due to the inability of the cavity system to produce temperatures high enough to totally evaporate the uranium sample before breakdown of the W heating filament. Note that Riciputi et al. [155] achieved a median

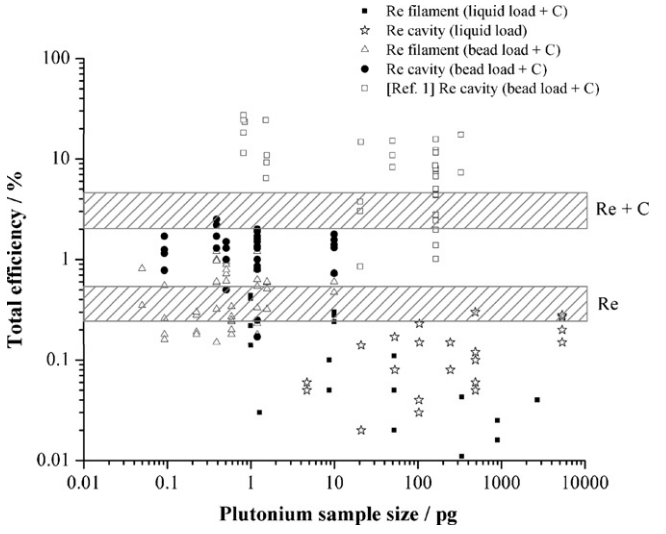

Fig. 2. Total efficiency (atoms loaded to ions detected) for plutonium as a function of analyte sample size using different loading techniques. Shaded areas indicate ionization efficiencies as predicated by the Saha–Langmuir equation. [Ref. 1] refers to [155].

efficiency of 5.8% ($n = 8$) for 100–500 pg uranium beads loaded into Re cavities using a predecessor ThermoFisher MC-TIMS generation and a similar cavity setup. Our inability to produce similar bead load cavity results for uranium with the setup used here is not understood at this point. Cavities with different inner diameters and depth were examined, as well as different distances of the tip of the cavity to the electron shield, but no improvement was achieved. Uranium efficiencies of up to 1–39% using cavity sources (see Table 3) are reported in the literature. But these values refer to ionization efficiencies and not to total efficiencies achievable when coupled to a mass spectrometer used for isotope ratio analysis—the main focus of this work. The diagonally shaded areas in Fig. 1

Table 3
Total efficiencies (atoms loaded to ions detected) for thermal ionization of actinides and fission products using various sample preparation and loading techniques; [#]only ionization efficiency; [$]average or median value.

Analytical method	Element, sample size/pg	Ion source	Sample form/additive	Total efficiency/%	Reference
Thermal ionization	Sr	W cavity	Carrier, 0.5–2 mg	44.1[$,#]	[151]
	Sr	Re, Ta, Re cavity		82[$,#], 58[$,#], 70[$,#]	[152]
	Sr/100 to 10^7	Re filament	Liquid	≤0.1	This work
	Sr/1700–4790	Re cavity	Liquid	0.15[$]	This work
	Sr	Ta cavity	Liquid	<0.1	This work
	Sr/5 to 10^4	Re cavity	Resin bead, carbon	2.5[$]	This work
	Tc/0.001–1	Re filament	Liquid, $Ca(NO_3)_2$ and La_2O_3 additives	>2	[111]
	Cs/0.47–0.67	Re filament	Resin bead, carbon	21.3[$]	This work
	Cs/2.3–29	Re cavity	Liquid	0.58[$]	This work
	Cs/500	Re cavity	Resin bead, carbon	14.3[$]	This work
	La	W cavity	Carrier, 0.5–2 mg	24.6[$,#]	[151]
	Nd/100–5000	Re filament	Liquids, H_3PO_4	0.61[$]	[165]
	Nd/2×10^8	W cavity	Oxide powder	15–20[#]	[153]
	Nd	W cavity	Carrier, 0.5–2 mg	42.9[$,#]	[151]
	Nd	W, Ta, Re cavity		80[$,#]	[150]
	Nd/100 to 10^7	Re filament	Liquid, no additive	≤1	This work
	Nd/200–1000	Re filament	Resin bead, carbon	2.1[$]	This work
	Nd/740–3310	Re, Ta cavity	Liquid	0.90[$], <0.05	This work
	Nd/20–2500	Re cavity	Resin bead, carbon	4.5[$]	This work
	Sm/4×10^8	W cavity	Oxide powder	≈50[#]	[153]
	Sm, Eu	W cavity	Carrier, 0.5–2 mg	65.9[$,#], 45.8[$,#]	[151]
	Eu/10^6 to 5×10^8	W cavity	Oxide powder/liquid	≈75[#]	[153]
	Dy/4×10^8	W cavity	Oxide powder	≈35[#]	[153]
	Dy	W cavity	Carrier, 0.5–2 mg	43.8[$,#]	[151]
	Dy	W, Ta, Re cavity		66[$,#]	[150]
	Lu/1.5×10^8	W cavity	Oxide powder	12.7[#]	[153]
	Th	Re filament	Liquid load	10^{-2} to 10^{-1}	[154,180,181]
	Th/25–5000	W cavity	Liquid, carbon	1.1–3[#]	[154]
	Th/100–300	Re filament	Liquid, carbon	4–6	[112]
	U	Re filament	Liquid load	10^{-2} to 10^{-1}	[154,180], this work
	U	Re filament	Liquid load, carbon	0.6–1.2[#]	[182]
	U/10^4	Re filament	Electrodeposition	0.015	[148]
	U/100–500	Re cavity	Resin bead, carbon	5.8[$]	[155]
	U/10^6	W cavity	Liquid, liquid + carbon	≈3.5[#], 8.5[#]	[153]
	U	Re, Ta, W cavity		39[$,#], 4.5[$,#], 15[$,#]	[152]
	U	W cavity	Carrier, 0.5–2 mg	15.1[$,#]	[151]
	U/7–605	Re filament	Cation resin bead, carbon	0.58[$]	This work
	U/7–71	Ta filament	Resin bead, carbon	0.02[$]	This work
	U/50–75	Re cavity	Liquid, carbon	0.021[$]	This work
	U	Ta cavity	Liquid, carbon	<0.025	This work
	Np/<10	Re filament	Resin beads, carbon	2[$]	[15]
	Np/100	W cavity	Liquids	≈4[#]	[153]
	Pu/<10	Re filament	Resin bead, carbon	5[$]	[15]
	Pu/0.005–0.016	Re filament	Resin bead, carbon	4–9	[159]
	Pu/0.82–330	Re cavity	Resin bead, carbon	8.0[$]	[155]
	Pu/100	W cavity	Liquid	≈8[#]	[153]
	Pu	W cavity	Carrier, 0.5–2 mg	16.2[$,#]	[151]
	Pu/pg size	Re filament	carbon	≈3	[178]
	Pu/0.05–10	Re filament	Resin bead, carbon	0.54[$]	This work, [90]
	Pu/4.7–5380	Re cavity	Liquid	0.13[$]	This work, [90]
	Pu/2690–5380	Ta cavity	Liquid	<0.01	This work
	Pu/0.093–10	Re cavity	Resin bead, carbon	1.33[$]	This work
	Am/0.174–0.29	Re filament	Resin bead, carbon	0.16[$]	This work
	Am/0.29	Re cavity	Resin bead, carbon	0.63[$]	This work
	Cm	W cavity	Carrier, 0.5–2 mg	8.8[$,#]	[151]
RIMS	(U), Pu/10^4			10^{-2}	[125]
	Np			3×10^{-6}[$]	[179]
	Pu/≈10			10^{-3}	[127]
AMS	U			10^{-2}	[122]
	Pu			≈10^{-2}	[121,185]
(MC)-SF-ICP-MS	U	MicroMist or Meinhardt nebulizer		0.004–0.03	[183,184]
	U	Nano-volume flow injection		≈0.1	[115]
	U, Pu	CETAC ARIDUS sample introduction system		≈0.1	[49]
	U	APEX sample introduction system		≈0.2	[184]
	U	CETAC ARIDUS sample introduction system		≈1	[120]
	Pu	APEX sample introduction system		1–1.5	L.R. Riciputi (unpublished results)

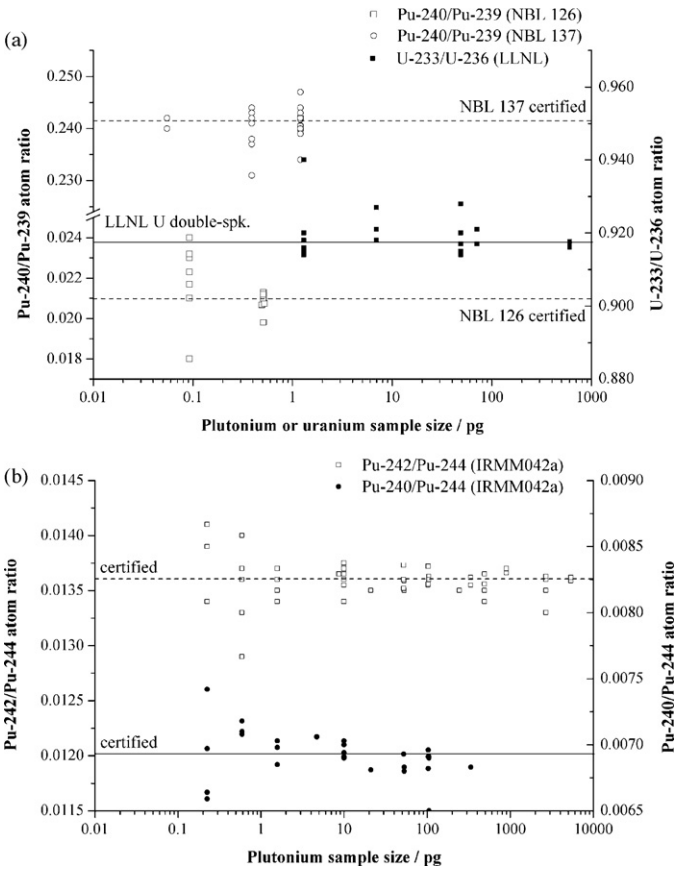

Fig. 3. Isotope ratio analysis (using secondary electron multiplier) of (a) plutonium (certified reference material NBL 126 and NBL 137), uranium ($^{233+236}$U double spike), and (b) of plutonium (certified reference material IRMM042a) using Re cavity or dimpled filament resin bead load techniques. No bias (e.g., mass fractionation) in the isotope ratio measurements was observed (within precision).

indicate the ionization efficiencies of uranium as predicted by the Saha–Langmuir equation for Re or Re with a carbon layer (Re + C). An operating temperature of T = 1800–2100 °C (temperature for filament analysis) and a first ionization potential of 6.194 eV were used in the calculations for uranium ionization efficiencies. For the uranium measurements reported here, the ^{233}U + ^{236}U double-spike was used. Uranium-233 and ^{236}U are an advantageous choice when studying efficiencies and detection limits, because the rhenium materials used for the filaments and cavities contain trace amounts of natural uranium and thus produces an enhanced background for isotopes ^{235}U and ^{238}U. Ta cavities, which have several orders of magnitude lower U content, were examined as an alternative to Re cavities. Unfortunately, the observed efficiencies using Ta cavities are a factor of 10–100 lower than those for Re cavities. Alternatively, the natural uranium blank level could potentially be reduced by using high purity Re materials (e.g., zone refined Re), which were not examined in this study.

Isotope ratio analysis for uranium sample sizes between 1 and 1000 pg were performed using a secondary electron multiplier (see Fig. 3a). At about 1 pg sample size (with about a 1:1 atom ratio ^{233}U/^{236}U), typical relative standard deviations of 1% are observed using bead load techniques onto filaments with carbon additive. Best achievable precisions are about RSD = 0.1% at about 1×10^5 cps ion beams when utilizing higher U sample sizes. No bias (e.g., mass fractionation) in the isotope ratio measurements were observed (within precision) using SEM. Background count rates at masses ^{233}U and ^{236}U are as low as 0.1–0.01 cps (measured using blank filaments with all chemical additives, i.e., background count rates stem from dark noise and potentially from atomic and/or molecular interferences; also measured at half-masses periodically during actual measurements).

The observed total efficiencies and background count rates result in a detection limit (3σ above background) of 1–10 fg $^{233+236}$U using Re cavity with liquid load method, and <0.1 fg (10^4 atoms to 10^5 atoms) $^{233+236}$U using a cation resin bead load onto Re + C filaments (see Table 2). The detection limits for ^{235}U and ^{238}U are of the order of 10^8 to 10^9 atoms, depending on the contribution of natural uranium from chemical blanks and the rhenium materials used. The detection limit for the ^{234}U isotope approaches low to sub-femtogram levels (10^5 atoms to 10^6 atoms), depending on the chemical blank and the purity of the Re material (^{234}U abundance in natural uranium is only 0.0055%). The lower ^{234}U detection limit – compared to ^{235}U and ^{238}U – is of advantage when analyzing enriched uranium samples, which can have ^{234}U abundances orders of magnitude higher than 0.0055%. Due to the ubiquitous natural uranium blank, isotope ratio analysis involving ^{234}U, ^{235}U, and ^{238}U at trace levels were not further investigated. Because of their frequent utilization for nuclear safeguards and forensics analysis, more studies in the future will have to be performed. An abundance sensitivity of 1×10^6 to 10^8 measured at atomic mass ^{236}U + 1 u when applying a ^{236}U beam can be achieved in low mass resolution mode using the SEM with RPQ. Therefore, ^{236}U signals will be affected by comparatively large ^{238}U beams.

3.2. Plutonium

For plutonium (see Fig. 2), a median total efficiency of 0.13% (n = 22) for 4.7–5380 pg Pu liquid loads into Re cavities without carbon, 0.54% (n = 45) for 0.05–10 pg Pu resin bead loads onto dimpled flat ribbon single Re + C filaments, and 1.33% (n = 30) for 0.093–10 pg Pu resin bead loads into Re cavities with carbon additive can be reported. This compares to a median total efficiency of 0.050% (n = 19) for plutonium liquid loads (1–2690 pg) onto normal flat ribbon single Re filaments with carbon. In contrast to the uranium results, no difference in the efficiencies for cation and anion resin beads for Pu was found. Using resin bead load techniques is about one to two orders of magnitudes more efficient than normal filament liquid loads (see Table 3). Riciputi et al. [155] achieved a median efficiency of 8.0% (n = 37) for 0.82–330 pg Pu beads loaded into Re cavities using an earlier ThermoFisher MC-TIMS instrument and a similar cavity setup. The difference of about a factor of 6 between the total efficiency for Pu cavity bead loads reported by [155] and the results reported here is not understood at this point. No improvement was achieved using cavities with different inner diameters and depth, as well as different distances of the tip of the cavity to the electron shield. Plutonium efficiencies of up to 16% using cavity sources have been reported in the literature (see Table 3), but these results refer mostly to ionization efficiencies (not total efficiencies) and isotope ratio analysis using a mass spectrometer are not discussed. To our knowledge, the highest efficiencies of 4–9% for plutonium isotope ratio analysis for a TIMS were reported by Smith et al. [159] using resin bead load techniques with carbon cover. The shaded areas in Fig. 2 indicate the ionization efficiencies of plutonium as predicted by the Saha–Langmuir equation for Re or Re with a carbon layer (Re + C). A filament temperature of T = 1750–2050 °C (signal temperature for filament analysis) and a first ionization potential of 6.026 eV were used in the calculations. The rhenium materials used in the filaments and cavities were tested and found to be Pu-free within detection limits.

Isotope ratio analysis for plutonium loads between 0.05 and 1.2 pg for NBL 126 and NBL 137 and between 0.225 and 5380 pg for IRMM042a were preformed using the secondary electron multiplier (see Fig. 3a and b). At about 1 pg plutonium load (minor Pu

isotope 10 fg), a relative standard deviation (RSD) of about 1–3% using bead load techniques can be reported. RSD of 0.1% can be achieved for larger sample sizes (at about 1×10^5 cps beam current). Isotope ratio measurements were performed on isotope amounts as low as 0.03 fg (minor isotope) using resin bead load techniques. The isotope ratio of $^{241}Pu/^{239}Pu$ was used to 'age-date' the NBL 126 and NBL 137 isotope standards utilizing the decay of ^{241}Pu ($T_{1/2}$ = 14.35 years). At 0.03, 4.4, and 13.5 fg ^{241}Pu per sample, an age (in years) of 1.2 ± 5.1, 1.9 ± 1.6, and 1.7 ± 0.7 was determined, respectively, compared to the reference age of 1.8 years (at date of analysis). The uncertainties (1σ) in the measured ages are relatively high due to counting statistics and a relatively young age compared to the half-life of ^{241}Pu. No bias (e.g., mass fractionation) in the measured isotope ratios was observed within the precision of the measurements when utilizing the SEM.

The SEM or MIC background count rate at Pu masses are about 0.1–1 cps, and can be as low as 0.01 cps (measured using blank filaments with all chemical additives, i.e., background count rates stem from dark noise and potentially from atomic and/or molecular interferences; also measured at half-masses periodically during actual measurements). The observed total efficiencies and background count rates result in a detection limit (3σ above background) of 0.1–1 fg $^{239-242,244}Pu$ using a Re cavity with liquid load; and <0.1 fg (10^4 atoms to 10^5 atoms) $^{239-242,244}Pu$ using resin bead load techniques (see Table 2). The abundance sensitivity is comparable to that reported for uranium utilizing SEM with RPQ.

Using multiple-ion counter (MIC) allows the simultaneous analysis of multiple isotopes (without losses due to duty cycle compared to SEM peak jumping) at ultra-low levels, resulting in better counting statistics, precision, and detection limits. The yield (ion detection efficiency) differs for the ion counters depending on the individual operating voltage and detector performances. The yield of each counter also tends to drift independently over both short and long timescales during analysis. Therefore, a suitable protocol to calibrate the MICs has to be established to perform accurate isotope ratio measurements. Two different calibration strategies can be applied: internal calibration or external calibration. External calibration can be utilized if the multiple-ion counters exhibit a negligible change in the individual yields (within desired precision) during the timeframe needed to analyze at least a single sample and one standard (i.e., one mass fractionation or quality control sample). In this case, the MICs can be calibrated relative to each other by bracketing one or more samples with a standard of known isotopic composition. If, on the other hand, the yield and performance of the MICs drift during the analysis time, external calibration cannot be adopted for accurate isotope ratio analysis. Instead, internal calibration has to be performed. In this case, the major isotope of the sample is rotated through all multiple-ion counters at a stable beam signal at certain time intervals during the analyses of the sample. This allows the calculation of the short-term drift of the individual MIC yields. The disadvantage of using internal calibration is that some of the acquisition time (thus sample amount) is used to calibrate the MICs during the measurement and thus results in decrease in the detection limit compared to the external calibration method.

To investigate which protocol is more suitable for the seven MICs installed on the utilized "Triton" MC-TIMS, a short- and long-term stability test of the MICs was performed (Fig. 4a and b). NBL 137 samples were loaded (3.6–18 pg of Pu) on normal single Re filament with carbon (unfilled symbols between 0 and 50 h in Fig. 4) and loaded as Pu resin beads (1.2 pg) into Re cavity with carbon (filled symbols between 150 and 200 h in Fig. 4). The isotope ratios $^{240}Pu/^{239}Pu$ (Fig. 4a), $^{241}Pu/^{239}Pu$ (Fig. 4b, triangular), and $^{242}Pu/^{239}Pu$ (Fig. 4b, squares) were monitored. Each sample was measured until full depletion of the ion signal, with all three isotope ratios ($^{240}Pu/^{239}Pu$, $^{241}Pu/^{239}Pu$, and $^{242}Pu/^{239}Pu$) monitored sequentially during the run. Thus, each sample yielded one data point for each of the three ratios reported. The two different types of sample loading (Re filaments with carbon, 0–50 h, versus resin bead load into cavity, 150–200 h) were employed to examine potential changes in the drift behavior of the MICs due to the physical changes in operation (e.g., applied voltages) when using the cavity ion source versus normal filament operation. The stability of the MIC is potentially sensitive to arcing (spikes in the operation voltages) caused in the ion source and lens regions, which can occasionally occur during cavity operations due to the larger thermal and electrical "stress". The beam intensity (ion dose) also has an effect on the stability of the yields and will therefore contribute to any changes in yields over time. No re-adjustment of the operation voltages of the MICs was required and the MICs high voltage was switched off overnight. Normal filament liquid loads yield RSD of about 0.6% (2 pg minor Pu isotope) and 1.6% (0.15 pg minor isotope), the cavity resin bead loads 1% (0.26 pg minor Pu isotope) and 1.8% (0.015 pg minor isotope). Note that bead loads are a factor of 10–100 more efficient than normal filament liquid loads. An even better RSD, as low as 0.1%, is achievable on MICs as demonstrated by Goldberg et al. [160] for uranium isotope ratio measurements using the same MC-TIMS generation, but at more favorable ratios ($^{235}U/^{238}U \approx 1$) and higher analyte concentration (10 pg U loads). Using multi-collector sector-field ICP-MS for isotope ratio analysis, Riciputi et al. (2007b) [161] report a RSD of about 1% (2σ) for minor plutonium isotope amounts of a few femtograms; Taylor et al. [162] a RSD of about 3% (2σ) for a few femtograms (minor plutonium isotope); and Snow and Friedrich [163] a RSD of about 0.2% (2σ) for uranium at a few picograms of the minor isotopes. In this study (see Fig. 4a and b), no difference in short-term (sample-to-sample) and long-term (within a day of operation or longer) behavior of the individual yields is apparent when comparing the measured precisions of the isotope ratios ($^{240}Pu/^{239}Pu$, $^{241}Pu/^{239}Pu$, and $^{242}Pu/^{239}Pu$). Also, no "jumps", i.e., sudden changes in the yields of the individual MICs, were observed. The isotope ratios exhibit no evident trends (e.g., systematically increasing or decreasing over time) and the scattering of the data points is well encompassed by their measured

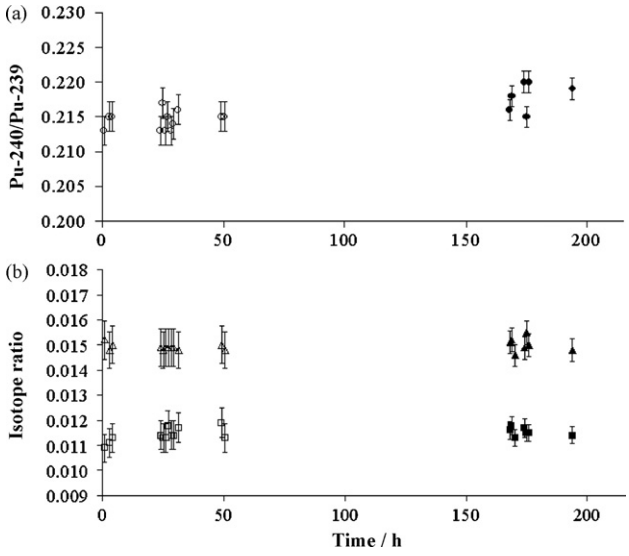

Fig. 4. Short-term and long-term stability test of the multiple-ion counters (MICs): isotope ratio analysis of (a) $^{240}Pu/^{239}Pu$ (circular), (b) $^{241}Pu/^{239}Pu$ (triangular), and $^{242}Pu/^{239}Pu$ (squares) of NBL 137 were measured for samples using normal liquid load onto Re flat ribbon filaments with carbon additive (0–50 h, unfilled symbols) and bead load into Re cavity with carbon additive (150–200 h, filled symbols). Each sample was measured until depletion of the ion signal, with all three isotope ratios ($^{240}Pu/^{239}Pu$, $^{241}Pu/^{239}Pu$, and $^{242}Pu/^{239}Pu$) monitored sequentially during the run, yielding one data point for each of the three ratios reported. The operation voltages of the MICs were not re-adjusted within the 200 h of operation.

uncertainties. Any potential drifts in the yields of the MICs appear to be too small to be resolved when compared to the uncertainties of the measurements of the individual samples (as indicated as uncertainty bars in Fig. 4a and b). These uncertainty bars reflect the pg sample sizes and, therefore, the relatively small number of total counts accumulated on the minor isotopes.

Thus, external calibration appears to be suitable for ultra-trace level analysis using discussed MICs with the "Triton" MC-TIMS, resulting in improved counting statistics for the minor isotopes at low abundances (compared to peak jumping the SEM) compensating potential additional sources of variability (uncertainty) from individual MIC yield drifts. Dark noise and ion detection yields of the individual MICs and the SEM are comparable. Riciputi et al. (2007b) [161] also report simultaneous multiple-ion counting analysis of small samples of uranium and plutonium using the ThermoFisher "Neptune" multi-collector sector-field ICP-MS. The results suggest that the performance of the MIC systems varies between the two platforms ("Triton" TIMS vs. "Neptune" ICP-MS), and may reflect the differences between the plasma and thermal ion source, single-focusing versus double-focusing geometry, and the performance of the MICs themselves.

Combined uranium and plutonium bead loads onto Re filaments were performed to study the change in total efficiency of plutonium when analyzed with excessive amounts of uranium. At an U/Pu ratio of 50, the total efficiency of Pu is depressed by about a factor of 2 compared to plutonium runs without uranium. Thus, a perfect U/Pu chemical separation is not strictly necessary. As can be seen from Fig. 5, plutonium signal intensity peaks at a temperature that is about 50 °C lower than the equivalent uranium temperature, allowing the sequential analysis of the isotope ratios of both elements in the same sample. No bias in the isotope ratios of the Pu reference material was observed due to the presence of excess uranium (see Fig. 5). An abundance sensitivity of typically 10^6 to 10^8 (using SEM with RPQ) enables accurate ^{239}Pu isotope ratio analysis even in the presences of several orders of magnitude more ^{238}U than ^{239}Pu. The same experiments were not repeated using bead loads into cavities, although the decrease in the efficiency for the minor element (Pu in this instance) will likely be even smaller due to the increased Re surface area of the cavity compared to the flat geometry of a filament.

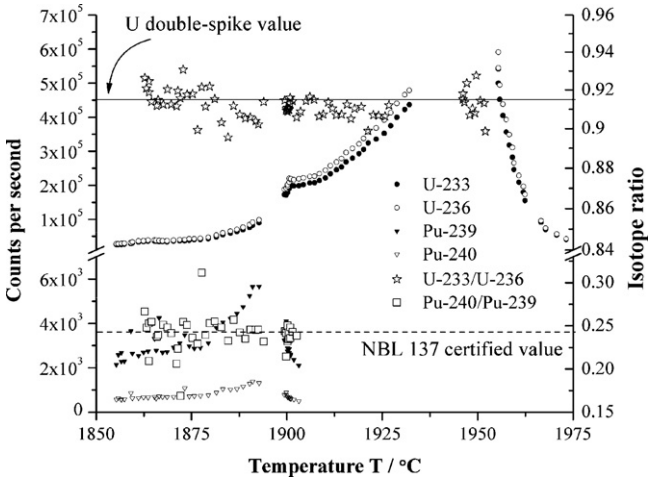

Fig. 5. Combined uranium and plutonium bead loads on Re filament at a U/Pu ratio of 50. The ionization efficiency of Pu is depressed by about a factor of 2 compared to plutonium runs without uranium. Maximum intensities of the plutonium signal are at a temperature that is about 50 °C lower than that for uranium, allowing the sequential isotope ratio analysis for both elements within the same run. No significant bias in the isotope ratio measurements of plutonium (e.g., due to excess uranium) was observed (within precision).

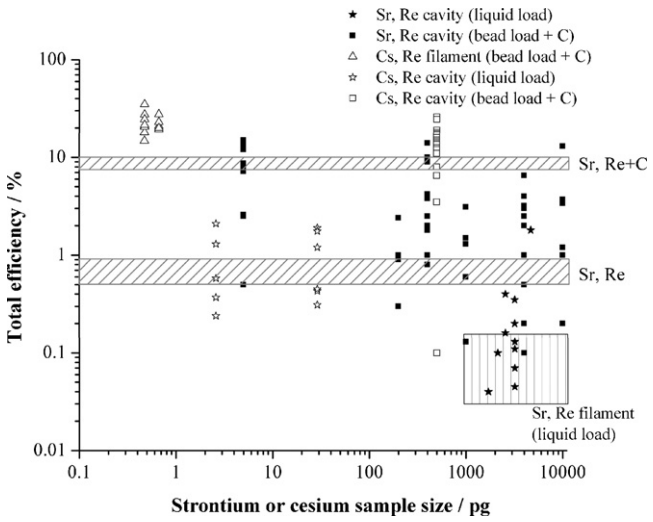

Fig. 6. Total efficiency (atoms loaded to ions detected) for Sr and Cs as a function of analyte sample size using different loading techniques. Diagonally shaded areas indicate ionization efficiencies as predicated by the Saha–Langmuir equation. The vertically shaded area indicates total efficiencies obtained using normal flat ribbon Re filaments and liquid load.

3.3. Americium

For americium (Fig. 1), a median total efficiency of 0.16% (n = 13) for 0.17–0.29 pg Am cation resin bead loads onto dimpled flat ribbon single Re filaments covered with carbon were observed. And a median total efficiency of 0.63% (n = 6) for 0.29 pg Am resin bead loads into Re cavities with carbon additive can be reported. No liquid loads with cavities were studied. The shaded areas in Fig. 1 indicate the ionization efficiencies of americium as predicted by the Saha–Langmuir equation for Re with carbon additive (Re + C). A filament operating temperature of T = 1750–2050 °C and a first ionization potential of 5.974 eV were used in the calculations. Americium blanks in the filament and cavity rhenium materials and reagents used were below detection limit. The available NIST 4223a (4332d) is essentially mono-isotopic (^{243}Am). Thus, no isotope ratio measurements for americium were performed, although precision and accuracies can be expected to be similar to those observed for uranium and plutonium. The SEM background count rate at masses ^{241}Am and ^{242}Am is typically between 1 and 0.01 cps. The achieved total efficiencies and background count rates result in a detection limit (3σ) of <0.1 fg (10^4 atoms to 10^5 atoms) $^{241-243}$Am using filament and cavity resin bead load techniques (see Table 2).

3.4. Strontium

For strontium (Fig. 6), a median total efficiency of 0.15% (n = 12) for 1700–4790 pg (Sr) liquid loads into Re cavities without carbon and 2.5% (n = 47) for 5 pg through 10 ng Sr resin bead loads into Re + C cavities can be reported. No stable ion beam signals could be achieved using resin bead load onto dimpled flat ribbon Re + C filaments. A total efficiency of about 0.15% for Sr for liquid loads into Re cavities is comparable to the ≤0.1% achieved with normal flat ribbon Re filament liquid loads (no TaO activator) (Fig. 6). Similar performance using a "Triton" MC-TIMS and single Re filaments has been reported by Font et al. [164] for strontium liquid loads. Sr efficiencies of up to 44–82% using cavity sources are reported in the literature (see Table 3), but these results refer mostly to ionization efficiencies (not total efficiencies) and isotope ratio analysis using a mass spectrometer are not discussed. Diagonally shaded areas in Fig. 6 indicate the ionization efficiencies of Sr as predicted by the Saha–Langmuir equation for Re or Re with a carbon layer

(Re + C). A filament operating temperature of T = 1300–1500 °C and a first ionization potential of 5.695 eV were used for the calculations. Multi-collector Faraday cup (FC) isotope ratio analysis for strontium loads between 0.1 and 1000 ng NBS 987 are summarized in Fig. 8 using both liquid load technique onto flat ribbon Re filaments or into Re cavities, and resin bead load into Re cavities.

Depending on the efficiency, a RSD ≈0.01% can be achieved at 0.1–1 ng Sr loads at 0.5 V ^{88}Sr Faraday cup signal (in static mode), and as low as RSD ≈0.001% for >10 ng Sr loads at 10–50 V ^{88}Sr. A precision of RSD ≈0.01% or better using cavity techniques or filament liquid loads combined with slow heating profiles is possible for total Sr samples of ≤1 ng. The method is limited by the Sr concentration of the reagent blanks. The RSD using SEM or MICs does not significantly exceed 0.1% at a count rate of about 1×10^5 cps ^{88}Sr, rendering ion counting mainly unsuitable for geolocation studies where precision of about RSD = 0.01% or better are desirable.

The observed total efficiencies and background count rates using SEM as detector yields a detection limit (3σ) of 0.1–1 fg ^{89,90}Sr using Re cavity or Re flat ribbon filament with liquid load and <0.1 fg (10^4 atoms to 10^5 atoms) ^{89,90}Sr using cavity resin bead load techniques. This is of particular interest in analysis of fission products ^{89}Sr and ^{90}Sr.

3.5. Cesium

For cesium (see Fig. 6), a median total efficiency of 0.58% (n = 11) for 2.3–29 pg Cs liquid loads into Re cavities without carbon, 21.3% (n = 14) for 0.47–0.67 pg Cs resin bead loads onto dimpled flat ribbon single Re filaments with carbon, and 14.3% (n = 18) for 500 pg Cs resin bead loads into Re + C cavities can be reported. Ionization efficiencies of Cs as predicted by the Saha–Langmuir equation for Re with or without a carbon layer (Re + C) are about 100% (filament temperature of T = 700–1000 °C, first ionization potential of 3.894 eV).

Natural Cs was used for the measurements, which is monoisotopic (^{133}Cs). Thus, no isotope ratio studies for cesium can be reported. The SEM background count rates at masses ^{134}Cs and ^{1345}Cs are as low as 0.1–0.01 cps. Reported total efficiencies and background count rates result in a detection limit (3σ above background) of <0.1 fg (10^4 atoms to 10^5 atoms) ^{134,135,137}Cs using resin bead load techniques. An abundance sensitivity of 10^6 to 10^7 at atomic mass ^{133}Cs + 1 u (when applying a ^{133}Cs beam) has been measured.

3.6. Neodymium

For neodymium (see Fig. 7), a median total efficiency of 0.90% (n = 11) for 740–3310 pg Nd liquid loads into Re cavities without carbon, 2.1% (n = 8) for 200–1000 pg Nd resin bead loads onto dimpled flat ribbon single Re filaments with carbon, and 4.5% (n = 46) for 20–2500 pg Nd resin bead loads into Re + C cavities can be reported. A total efficiency of 0.9% for Nd liquid loads into Re cavities is about comparable to normal flat ribbon Re filament liquid loads (≤1%). Similar results using a MC-TIMS (but using triple Re filaments) has been reported by Wakaki et al. [165] for Nd liquid loads. Nd efficiencies of up to 15–80% using cavity sources can be found in the literature (see Table 3), but these results refer mostly to ionization efficiencies (not total efficiencies) and isotope ratio analysis using a mass spectrometer are not discussed. Diagonally shaded areas in Fig. 7 indicate the ionization efficiencies of neodymium as predicted by the Saha–Langmuir equation for Re or Re with a carbon layer (Re + C). A filament temperature of T = 1600–1700 °C and a first ionization potential of 5.49 eV were used.

Isotope ratio analysis using multi-collector Faraday cups for neodymium liquid and bead loads between 0.7 and 300 ng La Jolla standard and 0.2 and 3 ng for "natural" Nd (ICP-MS/AAS standards) are summarized in Fig. 8. For favorable efficiencies, a RSD ≈0.01% can be achieved for 0.1–1 ng Nd loads at 0.3 V ^{142}Nd Faraday cup beam signal, and as low as RSD ≈0.001% for >10 ng Nd loads at 10–50 V ^{142}Nd beam signals (static mode). A precision of RSD ≈0.01% or better using cavity or filament techniques and slow heating profiles are suitable to resolve crucial geographical signatures at ≤1 ng Nd using Faraday cups. The method is limited by the concentration and isotopic composition of the chemical Nd blank. RSD using SEM or MICs does not significantly exceed 0.1% at a count rate of about 1×10^5 cps ^{142}Nd, rendering ion counting mainly not suitable for geolocation studies.

The observed total efficiencies and background count rates using SEM or MICs result in a detection limit (3σ above background) of about 1 pg Nd (all stable isotopes), significantly limited by the reagent blanks. In absence of this blank, a detection limit for bead load techniques comparable to that for Sr and Cs can be expected (<0.1 fg) using ion counting, which is based upon the observed total efficiencies. An abundance sensitivity of 10^6 to 10^7 measured at atomic mass ^{144}Nd + 1 u when applying a ^{144}Nd beam can be reported using SEM with RPQ, similar to that for Cs.

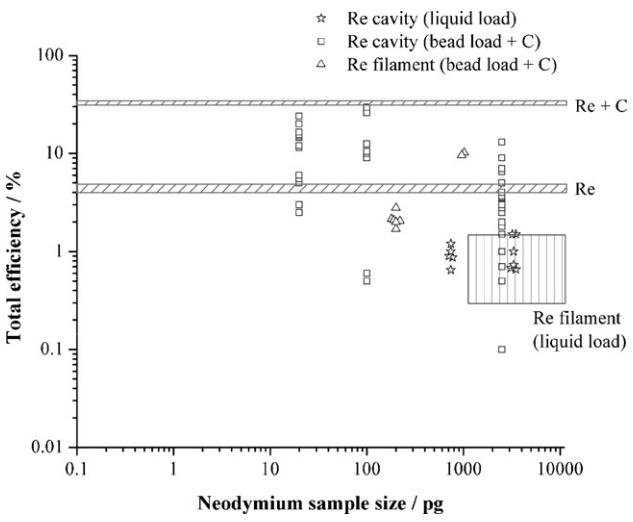

Fig. 7. Total efficiency (atoms loaded to ions detected) for Nd as a function of analyte sample size using different loading techniques. Diagonally shaded areas indicate ionization efficiencies as predicted by the Saha–Langmuir equation. The vertically shaded area indicates total efficiencies obtained using normal flat ribbon Re filaments.

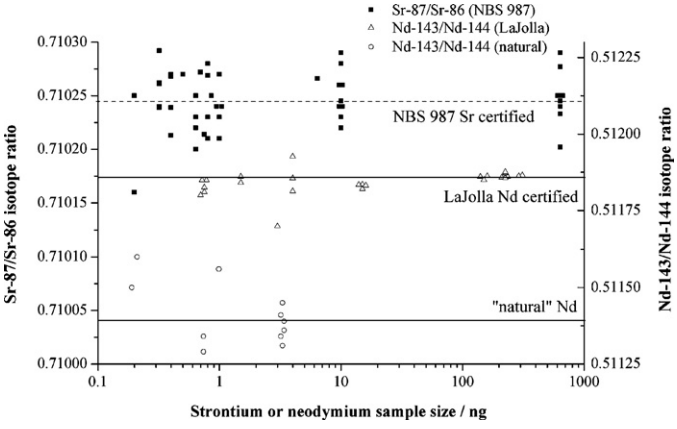

Fig. 8. Isotope ratio analysis using multi-collector Faraday cups for strontium (certified reference material NIST 987) and neodymium (La Jolla reference material and "natural" Nd) with liquid load and bead load techniques. No bias in the isotope ratio measurements was observed (within precision).

4. Conclusion

Total efficiencies (atoms loaded to ions detected) of up to 0.5–2% for U, Pu, and Am, and 1–30% for Sr, Cs, and Nd are observed when employing resin bead load techniques onto flat ribbon Re filaments or resin beads loaded into a millimeter-sized cavity drilled into a Re tube using a ThermoFisher "Triton" MC-TIMS. This results in detection limits (3σ above background) of <0.1 fg (10^4 atoms to 10^5 atoms) for $^{239-242+244}$Pu, $^{233+236}$U, $^{241-243}$Am, ^{89,90}Sr, and ^{134,135,137}Cs, and $\leq$1 pg for natural Nd isotopes (limited by the chemical processing blank) using secondary electron multiplier (SEM) or multiple-ion counters (MICs). To our knowledge, the detection limits reported herein for these Pu, Am, and U isotopes belong to the lowest reported limits for isotope ratio mass spectrometry analysis. It appears that the lowest ever reported isotope selective detection limit for plutonium mass spectrometry was demonstrated by Smith [159] using a TIMS with carbon-coated bead loads on Re filaments: "The detection limit of Pu-239 would be [...] perhaps a thousand atoms or lower"—total efficiencies of >1% are reported. Chemical processing blank of <10^4 atoms total Pu have been reported [15], thus an efficiency of >1% would enable the (statistically significant) detection of <10^4 atoms Pu if background count rates of about 0.01 cps can be maintained. Detection limits for ^{233}U, ^{236}U, Np and Am are potentially smaller due to lower chemical blanks.

Rhenium, compared to W or Ta, shows the best overall performance for thermal ionization mass spectrometry of actinides and fission products, as can be seen from Table 3. The improvement in efficiency and detection limits is mainly due to the use of resin bead load instead of normal liquid load, and the addition of carbon. This is because resin bead loads improve focus and ion transmission by reducing the geometrical size of the sample and act as reservoir and carbon source [146,149]. The carbon layer additionally enhances the work function of the ionizer materials (e.g., rhenium) and ion beams stability, and reduced isotope mass fractionation has been observed using carbon coating [149]. (The advent of nano-science has brought with it the discovery of new carbon compounds with surprising and sometimes unexpected physical and chemical properties at the nano-scale. These new carbon compounds, e.g., due to their surface-to-volume ratios at the nano-scale, might have great potential in their utilization as ionization enhancers for actinides.) A further advantage using resin bead loads is that resin beads adsorb specific analytes from a mixed actinide and fission product solution, thus adding an additional chemical separation step (but potentially increasing chemical processing blanks). The utilization of a cavity did not result in an enhancement of the ionization efficiency for U and Pu as expected and demonstrated by Riciputi et al. [155] using a predecessor ThermoFisher MC-TIMS generation and a very similar cavity setup; although improvements for Am and Nd can be reported. The reason for the difference in the U and Pu efficiencies reported by [155] and reported here is not understood at this point.

As with essentially all analytical tasks, a suitable analytical instrument and procedure has to be chosen. "It is generally recognized that there is no one single type of mass spectrometer that fulfils all of the requirements for measuring all varying sample types and compositions encountered in a laboratory" [64]. The advantages of MC-TIMS, i.e., comparably high abundance sensitivities, small molecular interferences, high precision and accuracy, low detection limits, and oligo-element capability, make it together with MC-SF-ICP-MS one of the most versatile and suitable instruments for isotope ratio analysis. The studies on actinide, fission product, and geolocator analyses presented here further probe and help understand capabilities and limitations of this versatile analytical technology.

Acknowledgment

We like to thank the two reviewers for their helpful comments. Research sponsored by the Office of Non-Proliferation Research and Engineering (NA-22), National Nuclear Security Administration (NNSA), U.S. Department of Energy, under contract DE-AC05-00OR22725 with Oak Ridge National Laboratory, managed and operated by UT-Battelle, LLC. The submitted manuscript was authored by a contractor of the U.S. Government under contract No. DE-AC05 00OR22725. Accordingly, the U.S. Government retains a nonexclusive, royalty-free license to publish or reproduce the published form of this contribution, or allow others to do so, for U.S. Government purposes.

References

[1] D.L. Donohue, Journal of Alloys and Compounds 271–273 (1998) 11–18.
[2] K. Mayer, M. Wallenius, I. Ray, Analyst 130 (2005) 433–441.
[3] K.J. Moody, I.D. Hutcheon, P.M. Grant, Nuclear Forensic Analysis, CRC Press, Taylor & Francis Group, 2005.
[4] S. Usuda, K. Yasuda, Y. Saito-Kokubu, F. Esaka, C.-G. Lee, M. Magara, S. Sakurai, K. Watanabe, F. Hirayama, H. Fukuyama, K.T. Esaka, K. Iguchi, Y. Miyamoto, J.-Y. Chai, International Journal of Environmental Analytical Chemistry 86 (2006) 663–675.
[5] K. Mayer, M. Wallenius, T. Fanghänel, Journal of Alloys and Compounds 444 (2007) 50–56.
[6] D.M. Taylor, Applied Radiation and Isotopes 46 (1995) 1245–1252.
[7] W.C. Inkret, D.W. Efurd, G. Miller, D.J. Rokop, T.M. Benjamin, International Journal of Mass Spectrometry 178 (1998) 113–120.
[8] D. Lewis, G. Miller, C.J. Duffy, D.W. Efurd, W.C. Inkret, S.E. Wagner, Journal of Radioanalytical and Nuclear Chemistry 249 (2001) 115–120.
[9] K.G.W. Inn, D. McCurdy, L. Kuruvilla, N.M. Barss, R. Pietrzak, E. Kaplan, W. Inkret, W. Efurd, D. Rokop, D. Lewis, P. Gauthier, R.T. Bell III, Journal of Radioanalytical and Nuclear Chemistry 249 (2001) 121–131.
[10] D. McCurdy, Z. Lin, K.G.W. Inn, R. Bell III, S. Wagner, D.W. Efurd, R. Steiner, C. Duffy, T.F. Hamilton, T.A. Brown, A.A. Marchetti, Journal of Radioanalytical and Nuclear Chemistry 263 (2005) 447–455.
[11] D.W. Efurd, R.E. Steiner, F.R. Roensch, S.E. Glover, J.A. Musgrave, Journal of Radioanalytical and Nuclear Chemistry 263 (2005) 387–391.
[12] E.P. Hardy, P.W. Krey, H.L. Volchok, Nature 241 (1973) 444–445.
[13] M. Koide, K.K. Bertine, T.J. Chow, E.D. Goldberg, Earth and Planetary Science Letters 72 (1985) 1–8.
[14] R.J. Pentreath, Applied Radiation and Isotopes 46 (1995) 1279–1285.
[15] T.M. Beasley, J.M. Kelly, T.C. Maiti, L.A. Bond, Journal of Environmental Radioactivity 38 (1998) 133–146.
[16] P.R. Danesi, A. Bleise, W. Burkart, T. Cabianca, M.J. Campbell, M. Makarewicz, J. Moreno, C. Tuniz, M. Hotchkis, Journal of Environmental Radioactivity 64 (2003) 121–131.
[17] A.H. Mohagheghi, S.T. Shanks, J.A. Zigmond, G.L. Simmons, S.L.A. Ward, Journal of Radioanalytical and Nuclear Chemistry 263 (2005) 189–195.
[18] J.H. Buchmann, J.E.S. Sarkis, M.H. Kakazu, C. Rodrigues, Journal of Radioanalytical and Nuclear Chemistry 270 (2006) 291–298.
[19] S. Bürger, R. A. Buda, H. Geckeis, G. Huber, J. V. Kratz, P. Kunz, C. Lierse von Gostomski, G. Passler, A. Remmert, N. Trautmann, Radioactivity in the Environment, vol. 8, 2006, p. 581, ISSN 1569-4860.
[20] R. Leifert, Z.R. Juzdan, W.R. Kelly, J.D. Fassett, K.R. Eberhardt, Science 238 (1987) 512–514.
[21] S. Salaymeh, S.C. Lee, P.K. Kuroda, Journal of Radioanalytical and Nuclear Chemistry 111 (1987) 147–155.
[22] P.I. Mitchell, L. León Vintró, H. Dahlgaard, C. Gascó, J.A. Sánchez-Cabeza, The Science of the Total Environment 202 (1997) 147–153.
[23] R. Chiappini, F. Pointurier, J.C. Millies-Lacroix, G. Lepetit, P. Hemet, The Science of the Total Environment 237/238 (1999) 269–276.
[24] I. Friberg, Applied Radiation and Isotopes 50 (1999) 365–373.
[25] A. Kudo, Journal of Environmental Radioactivity 57 (2001) 81–85.
[26] V. Zheltonozhsky, K. Mück, M. Bondarkov, Journal of Environmental Radioactivity 57 (2001) 151–166.
[27] Y. Saito-Kokubu, F. Esaka, K. Yasuda, M. Magara, Y. Miyamoto, S. Sakurai, S. Usuda, H. Yamazaki, S. Yoshikawa, S. Nagaoka, Applied Radiation and Isotopes 65 (2007) 465–468.
[28] A.B. Kersting, D.W. Efurd, D.L. Finnegan, D.J. Rokop, D.K. Smith, L. Thompson, Nature 397 (1999) 56–59.
[29] G.R. Choppin, Radiochimica Acta 91 (2003) 645–649.
[30] B. Kuczewski, C.M. Marquardt, A. Seibert, H. Geckeis, J.V. Kratz, N. Trautmann, Analytical Chemistry 75 (2003) 6769–6774.
[31] C.M. Marquardt, A. Seibert, R. Artinger, M. Denecke, B. Kuczewski, D. Schild, T. Fanghänel, Radiochimica Acta 92 (2004) 617–623.
[32] H. Geckeis, T. Schäfer, W. Hauser, Th. Rabung, T. Missana, C. Degueldre, A. Möri, J. Eikenberg, Th. Fierz, W.R. Alexander, Radiochimica Acta 92 (2004) 765–774.

[33] A.P. Novikov, S.N. Kalmykov, S. Utsunomiya, R.C. Ewing, F. Horreard, A. Merkulov, S.B. Clark, V.V. Tkachev, B.F. Myasoedov, Science 314 (2006) 638–641.
[34] C. Ambard, A. Delorme, N. Baglan, J. Aupiais, F. Pointurier, C. Madic, Radiochimica Acta 93 (2005) 665–673.
[35] S. Bürger, N.L. Banik, R.A. Buda, J.V. Kratz, B. Kuczewski, N. Trautmann, Radiochimica Acta 95 (2007) 433–438.
[36] M.S. Baxter, S.W. Fowler, P.P. Povinec, Applied Radiation and Isotopes 46 (1995) 1213–1223.
[37] R.J. Cornett, T. Eve, A.E. Docherty, E.L. Cooper, Applied Radiation and Isotopes 46 (1995) 1239–1243.
[38] F. Gauthier-Lafaye, P. Holliger, P.-L. Blanc, Geochimica et Cosmochimica Acta 60 (1996) 4831–4852.
[39] K. Hirose, M. Aoyama, T. Miyao, Y. Igarashi, Journal of Radioanalytical and Nuclear Chemistry 248 (2001) 771–776.
[40] G.T. Seaborg, M.L. Perlman, Journal of American Chemical Society 70 (1948) 1571–1573.
[41] C.S. Garner, N.A. Bonner, G.T. Seaborg, Journal of American Chemical Society 70 (1948) 3453–3454.
[42] D.C. Hoffman, F.O. Lawrence, J.L. Mewherter, F.M. Rourke, Nature 234 (1971) 132–134.
[43] E.C. Alexander Jr., R.S. Lewis, J.H. Reynolds, M.C. Michel, Science 172 (1971) 837–840.
[44] G. Herrmann, Physica Scripta 10A (1974) 71–76.
[45] S. Fried, A.M. Friedman, E. Callis, F. Schreiner, J. Hines, K. Orlandini, D. Nelson, E.O. Olsen, Nature 313 (1985) 301–303.
[46] J.Y. Chai, Y. Miyamoto, Y. Kokubu, M. Magara, S. Sakurai, S. Usuda, Y. Oura, M. Ebihara, Journal of Radioanalytical and Nuclear Chemistry 272 (2007) 397–401.
[47] L.W. Green, C.H. Knight, T.H. Longhurst, R.M. Cassidy, Analytical Chemistry 56 (1984) 696–700.
[48] L.W. Green, N.L. Elliot, F.C. Miller, J.J. Leppinen, Journal of Radioanalytical and Nuclear Chemistry 131 (1989) 299–309.
[49] S.F. Boulyga, J.S. Becker, Journal of Analytical Atomic Spectrometry 17 (2002) 1143–1147.
[50] V.P. Mironov, J.L. Matusevich, V.P. Kudrjashov, P.I. Ananich, V.V. Zhuravkov, S.F. Boulyga, J.S. Becker, Radiochimica Acta 93 (2005) 781–784.
[51] S.F. Wolf, D.L. Bowers, J.C. Cunnane, Journal of Radioanalytical and Nuclear Chemistry 263 (2005) 581–586.
[52] D.C. Gerlach, J.B. Cliff, D.E. Hurley, B.D. Reid, W.W. Little, Applied Surface Science 252 (2006) 7041–7044.
[53] G.S. Chang, J.M. Ryskamp, Nuclear Technology 129 (2000) 326–337.
[54] S. Portier, S. Brémier, C.T. Walker, International Journal of Mass Spectrometry 263 (2007) 113–126.
[55] A.O. Nier, Physical Review 55 (1939) 150–153.
[56] L.A. Dietz, C.F. Pachucki, G.A. Land, Analytical Chemistry 34 (1962) 709–710.
[57] S.K. Aggarwal, Radiochimica Acta 94 (2006) 397–401.
[58] G.R. Hertel, The Journal of Chemical Physics 47 (1967) 335–336.
[59] G.R. Hertel, The Journal of Chemical Physics 48 (1968) 2053–2058.
[60] D.H. Smith, G.R. Hertel, The Journal of Chemical Physics 51 (1969) 3105–3107.
[61] D.H. Smith, The Journal of Chemical Physics 54 (1971) 1424–1425.
[62] N. Erdmann, M. Nunnemann, K. Eberhardt, G. Herrmann, G. Huber, S. Köhler, J.V. Kratz, G. Passler, J.R. Peterson, N. Trautmann, A. Waldek, Journal of Alloys and Compounds 271–273 (1998) 837–840.
[63] J.R. de Laeter, H.S. Peiser, Analytical and Bioanalytical Chemistry 375 (2003) 62–72.
[64] S. Richter, S.A. Goldberg, International Journal of Mass Spectrometry 229 (2003) 181–197.
[65] J.K. Böhlke, J.R. De Laeter, P. De Bièvre, H. Hidaka, H.S. Peiser, K.J.R. Rosman, P.D.P. Taylor, Journal of Physical and Chemical Reference Data 34 (2005) 57.
[66] A.O. Nier, E.T. Booth, J.R. Dunning, A.V. Grosse, Physical Review 57 (1940) 546.
[67] J.R. de Laeter, Mass Spectrometry Reviews 15 (1996) 261–281.
[68] G.A. Cowan, H.H. Adler, Geochimica et Cosmochimica Acta 40 (1976) 1487–1490.
[69] D.H. Smith, J.R. Walton, H.S. McKown, R.L. Walker, J.A. Carter, Analytica Chimica Acta 142 (1982) 355–359.
[70] D.J. Rokop, D.W. Efurd, T.M. Benjamin, J.H. Cappis, J.W. Chamberlin, H. Poths, F.R. Roensch, Journal of the Royal Society of Western Australia 79 (1996) 85–90.
[71] M. Betti, G. Tamborini, L. Koch, Analytical Chemistry 71 (1999) 2616–2622.
[72] S. Richter, A. Alonso, W. De Bolle, R. Wellum, P.D.P. Taylor, International Journal of Mass Spectrometry 193 (1999) 9–14.
[73] D. Berkovits, H. Feldstein, S. Ghelberg, A. Hershkowitz, E. Navon, M. Paul, Nuclear Instruments and Methods in Physics Research B 172 (2000) 372–376.
[74] I.W. Croudace, P.E. Warwick, R.N. Taylor, A.B. Cundy, Environmental Science and Technology 34 (2000) 4496–4503.
[75] S.F. Boulyga, C. Testa, D. Desideri, J.S. Becker, Journal of Analytical Atomic Spectrometry 16 (2001) 1283–1289.
[76] T. Warneke, I.W. Croudace, P.E. Warwick, R.N. Taylor, Earth and Planetary Science Letters 203 (2002) 1047–1057.
[77] M. Wallenius, K. Mayer, I. Ray, Forensic Science International 156 (2006) 55–62.
[78] L. Pajo, A. Schubert, L. Aldave, L. Koch, Y.K. Bibilashvili, Y.N. Dolgov, N.A. Chorokhov, Journal of Radioanalytical and Nuclear Chemistry 250 (2001) 79–84.
[79] A. Ciurapinski, J. Parus, D. Donohue, Journal of Radioanalytical and Nuclear Chemistry 251 (2002) 345–352.
[80] I.L.F. Ray, A. Schubert, M. Wallenius, Advances in destructive and non-destructive analysis for environmental monitoring and nuclear forensics, IAEA-CN-98/82P, 2003, 371.
[81] B. Salbu, K. Janssens, O.C. Linda, K. Proost, L. Gijsels, P.R. Danesi, Journal of Environmental Radioactivity 78 (2005) 125–135.
[82] O.C. Lind, B. Salbu, K. Janssens, K. Proost, H. Dahlgaard, Journal of Environmental Radioactivity 81 (2005) 21–32.
[83] R. Zeisler, D.L. Donohue, Journal of Radioanalytical and Nuclear Chemistry 194 (1995) 229–235.
[84] S. Bürger, L.R. Riciputi, D.A. Bostick, Journal of Radioanalytical and Nuclear Chemistry 274 (2007) 491–505.
[85] S. Bürger, L.R. Riciputi, D.A. Bostick, W.S. Kinman, Isotopic and Elemental Analysis of Nuclear Materials by Mass Spectrometry, American Chemical Society, Fall Meeting, Boston, 2007.
[86] J. Švedkauskaité-LeGore, K. Mayer, S. Millet, A. Nicholl, G. Rasmussen, D. Baltrūnas, Radiochimica Acta 95 (2007) 601–605.
[87] E. Keegan, S. Richter, I. Kelly, H. Wong, P. Gadd, H. Kuehn, A. Alonso-Munoz, Applied Geochemistry 23 (2008) 765–777.
[88] L. Pajo, K. Mayer, L. Koch, Fresenius Journal of Analytical Chemistry 371 (2001) 348–352.
[89] G. Tamborini, M. Wallenius, O. Bildstein, L. Pajo, M. Betti, Microchimica Acta 139 (2002) 185–188.
[90] S. Bürger, L.R. Riciputi, S. Turgeon, D. Bostick, E. McBay, M. Lavelle, Journal of Alloys and Compounds 444–445 (2007) 660–662.
[91] D.L. Miller, L.R. Riciputi, S. Bürger, J. Horita, D.A. Bostick, Analysis of Concentrated Uranium Ores Using Stable Isotopes and Elemental Concentrations, American Geophysical Union, Fall Meeting, San Francisco, 2006.
[92] M. Wallenius, K. Mayer, Fresenius Journal of Analytical Chemistry 366 (2000) 234–238.
[93] M. Wallenius, G. Tamborini, L. Koch, Radiochimica Acta 89 (2001) 55–58.
[94] M. Wallenius, A. Morgenstern, C. Apostolidis, K. Mayer, Analytical and Bioanalytical Chemistry 374 (2002) 379–384.
[95] R.P. Keegan, R.J. Gehrke, Applied Radiation and Isotopes 59 (2003) 137–143.
[96] U. Nygren, H. Ramebäck, C. Nilsson, Journal of Radioanalytical and Nuclear Chemistry 272 (2007) 45–51.
[97] J.C. Vogel, B. Eglington, J.M. Auret, Nature 346 (1990) 747–749.
[98] K.A. Hobson, Oecologia 120 (1999) 314–326.
[99] J.R. Ehleringer, J.F. Casale, M.J. Lott, V.L. Ford, Nature 408 (2000) 311–312.
[100] B.L. Beard, C.M. Johnson, Journal of Forensic Sciences 45 (2000) 1049–1061.
[101] C. Tuniz, U. Zoppi, M.A.C. Hotchkis, Nuclear Instruments and Methods in Physics Research B 213 (2004) 469–475.
[102] S. Kelly, K. Heaton, J. Hoogewerff, Trends in Food Science and Technology 16 (2005) 555–567.
[103] S. Benson, C. Lennard, P. Maynard, C. Roux, Forensic Science International 157 (2006) 1–22.
[104] M.G. Inghram, Annual Review of Nuclear Science 4 (1954) 81–92.
[105] K.G. Heumann, International Journal of Mass Spectrometry and Ion Processes 118/119 (1992) 575–592.
[106] K.G. Heumann, S. Eisenhut, S. Gallus, E.H. Hebeda, R. Nusko, A. Vengoshand, T. Walczyk, Analyst 120 (1995) 1291–1299.
[107] K.G. Heumann, S.M. Gallus, G. Rädlinger, J. Vogl, Journal of Analytical Atomic Spectrometry 13 (1998) 1001–1008.
[108] F.A. White, T.L. Collins, F.M. Rourke, Physical Review 101 (1956) 1786–1791.
[109] D.H. Smith, W.H. Christie, H.S. McKown, R.L. Walkek, G.R. Hertel, International Journal of Mass Spectrometry and Ion Physics 10 (1972/1973) 343–351.
[110] R.S. Strebin, D.M. Robertson, Analytica Chimica Acta 91 (1977) 267–272.
[111] D.J. Rokop, N.C. Schroeder, K. Wolfsberg, Analytical Chemistry 62 (1990) 1271–1274.
[112] T.M. Esat, International Journal of Mass Spectrometry and Ion Processes 148 (1995) 159–170.
[113] J. Toole, A.S. Hursthouse, P. McDonald, K. Sampson, M.S. Baxter, R.D. Scott, K. McKay, The determination of actinides in environmental samples by ICP-MS, in: K.E. Jarvis, A.L. Gray, J.G. Williams (Eds.), Plasma Source Mass Spectrometry, RSC, London, 1990.
[114] J.F. Wacker, N.A. Wogman, K.B. Olsen, S.L. Petersen, O.T. Farmer, J.M. Kelley, G.C. Eiden, T.C. Maiti, Ultratrace analysis of uranium and plutonium by mass spectrometry, in: Advances in Destructive and Non-destructive Analysis for Environmental Monitoring and Nuclear Forensics, IAEA-CN-98/18, 2003, pp. 115–120.
[115] D. Schaumlöffel, P. Giusti, M.V. Zoriy, C. Pickhardt, J. Szpunar, R. Łobiński, J.S. Becker, Journal of Analytical Atomic Spectrometry 20 (2005) 17–21.
[116] J.B. Truscott, P. Jones, B.E. Fairman, E.H. Evans, Analytica Chimica Acta 433 (2001) 245–253.
[117] I. Rodushkin, P. Lindahl, E. Holm, P. Roos, Nuclear Instruments and Methods in Physics Research A 423 (1999) 472–479.
[118] R.N. Taylor, T. Warneke, J.A. Milton, I.W. Croudace, P.E. Warwick, R.W. Nesbitt, Journal of Analytical Atomic Spectrometry 16 (2001) 279–284.
[119] Y. Muramatsu, S. Yoshida, A. Tanaka, Journal of Radioanalytical and Nuclear Chemistry 255 (2003) 477–480.
[120] D.L. Hoffmann, International Journal of Mass Spectrometry 275 (2008) 75–79.
[121] L.K. Fifield, R.G. Cresswell, M.L. di Tada, T.R. Ophel, J.P. Day, A.P. Clacher, S.J. King, N.D. Priest, Nuclear Instruments and Methods in Physics Research B 117 (1996) 295–303.

[122] X.L. Zhao, L.R. Kilius, A.E. Litherland, T. Beasley, Nuclear Instruments and Methods in Physics Research B 126 (1997) 297–300.
[123] J.E. McAninch, T.F. Hamilton, T.A. Brown, T.A. Jokela, J.P. Knezovich, T.J. Ognibene, I.D. Proctor, M.L. Roberts, E. Sideras-Haddad, J.R. Southon, J.S. Vogel, Nuclear Instruments and Methods in Physics Research B 172 (2000) 711–716.
[124] L.K. Fifield, H.-A. Synal, M. Suter, Nuclear Instruments and Methods in Physics Research B 223–224 (2004) 802–806.
[125] D.L. Donohue, D.H. Smith, J.P. Young, H.S. McKown, C.A. Pritchard, Analytical Chemistry 56 (1984) 379–381.
[126] M. Nunnemann, N. Erdmann, H.-U. Hasse, G. Huber, J.V. Kratz, P. Kunz, A. Mansel, G. Passler, O. Stetzer, N. Trautmann, A. Waldek, Journal of Alloys and Compounds 271–273 (1998) 45–48.
[127] C. Grüning, G. Huber, P. Klopp, J.V. Kratz, P. Kunz, G. Passler, N. Trautmann, A. Waldek, K. Wendt, International Journal of Mass Spectrometry 235 (2004) 171–178.
[128] N. Trautmann, G. Passler, K.D.A. Wendt, Analytical and Bioanalytical Chemistry 378 (2004) 348–355.
[129] D.C. Duckworth, C.M. Barshick, D.A. Bostick, D.H. Smith, Applied Spectroscopy 47 (1993) 243–245.
[130] L.R. Riciputi, D.C. Duckworth, C.M. Barshick, D.H. Smith, International Journal of Mass Spectrometry and Ion Processes 146/147 (1995) 55–64.
[131] M. Betti, International Journal of Mass Spectrometry 242 (2005) 169–182.
[132] C.G. Lee, K. Iguchi, J. Inagawa, D. Suzuki, F. Esaka, M. Magara, S. Sakurai, K. Watanabe, S. Usuda, Journal of Radioanalytical and Nuclear Chemistry 272 (2007) 299–302.
[133] C. Leloup, P. Marty, D. Dall'Ava, M. Perdereau, Journal of Analytical Atomic Spectrometry 12 (1997) 945–950.
[134] R.E. Russo, X. Mao, H. Liu, J. Gonzales, S.S. Mao, Talanta 57 (2002) 425–451.
[135] S.F. Boulyga, D. Desideri, M.A. Meli, C. Testa, J.S. Becker, International Journal of Mass Spectrometry 226 (2003) 329–339.
[136] S. Bürger, L.R. Riciputi, D.A. Bostick, D.C. Duckworth, Characterization of Nuclear Materials Using Time-of-Flight ICP-MS, Federation of Analytical Chemistry and Spectroscopy Societies, Annual Meeting, Lake Buena Vista, Florida, 2006.
[137] M. Joseph, P. Manoravi, N. Sivakumar, R. Balasubramanian, International Journal of Mass Spectrometry 253 (2006) 98–103.
[138] S.F. Boulyga, M. Tibi, K.G. Heumann, Analytical and Bioanalytical Chemistry 378 (2004) 342–347.
[139] S.F. Boulyga, K.G. Heumann, Journal of Analytical Atomic Spectrometry 19 (2004) 1501–1503.
[140] G.L. Klunder, P.M. Grant, B.D. Andersen, R.E. Russo, Analytical Chemistry 76 (2004) 1249–1259.
[141] G.L. Klunder, Trace Chemical Detection using Laser Ablation Ion-Storage Time-of-Flight Mass Spectrometry, Federation of Analytical Chemistry and Spectroscopy Societies, Annual Meeting, Lake Buena Vista, Florida, 2006.
[142] J. González, C. Liu, X. Mao, R.E. Russo, Journal of Analytical Atomic Spectrometry 19 (2004) 1165–1168.
[143] J. González, S.H. Dundas, C.Y. Liu, X. Mao, R.E. Russo, Journal of Analytical Atomic Spectrometry 21 (2006) 778–784.
[144] J. De Laeter, M.D. Kurz, Journal of Mass Spectrometry 41 (2006) 847–854.
[145] D.H. Smith, The Journal of Chemical Physics 55 (1971) 4152–4154.
[146] D.H. Smith, W.H. Christie, R.E. Eby, International Journal of Mass Spectrometry and Ion Physics 36 (1980) 301–316.
[147] D.H. Smith, J.A. Carter, International Journal of Mass Spectrometry and Ion Physics 40 (1981) 211–215.
[148] D.J. Rokop, R.E. Perrin, G.W. Knobeloch, V.M. Armijo, W.R. Shields, Analytical Chemistry 54 (1982) 957–960.
[149] D.H. Smith, Thermal ionization mass spectrometry, in: C.M. Barshick, D.C. Duckworth, D.H. Smith (Eds.), Inorganic Mass Spectrometry, Marcel Dekker, Inc., New York, 2000.
[150] G.J. Beyer, E. Herrmann, A. Piotrowski, V.J. Raiko, H. Tyrroff, Nuclear Instruments and Methods 96 (1971) 437–439.
[151] P.G. Johnson, A. Bolson, C.M. Henderso, Nuclear Instruments and Methods 106 (1973) 83–87.
[152] R. Kirchner, Nuclear Instruments and Methods in Physics Research A 292 (1990) 203–208.
[153] Y. Duan, R.E. Danen, X. Yan, R. Steiner, J. Cuadrado, D. Wayne, V. Majidi, J.A. Olivares, Journal of the American Society for Mass Spectrometry 10 (1999) 1008–1015.
[154] D.M. Wayne, W. Hang, D.K. McDaniel, R.E. Fields, E. Rios, V. Majidi, International Journal of Mass Spectrometry 216 (2002) 41–57.
[155] L.R. Riciputi, K.B. Ingeneri, P.M.L. Hedberg, Advances in destructive and non-destructive analysis for environmental monitoring and nuclear forensics, in: Conference Proceeding IAEA-CN-98/25P, 2003, p. 347.
[156] L.R. Riciputi, K.B. Ingeneri, P.M.B. Hedberg, Utilization of cavity ion source thermal ionization mass spectrometry for the analysis of uranium and plutonium isotope ratios, in preparation.
[157] Triton Hardware Manual, ThermoFinnigan, Rev. 0, Issue 12/2002 (2002).
[158] Handbook of Chemistry and Physics, 65th edition, CRC, 1984.
[159] D.H. Smith, H.S. McKown, D.T. Bostick, R.M. Coleman, D.C. Duckworth, R.L. McPherson, Analysis of Femtogram-sized Plutonium Samples, Oak Ridge National Laboratory, 1994, ORNL/TM-1263.
[160] S.A. Goldberg, S. Richter, R. Essex, P. Mason, Improved environmental and forensics measurements using multiple ion counters, in: Advances in Destructive and Non-destructive Analysis for Environmental Monitoring and Nuclear Forensics, IAEA-CN-98/23, 2003, pp. 155–164.
[161] L.R. Riciputi, D.A. Bostick, S. Bürger, E. McBay, Multiple-ion Counting Inductively-coupled Plasma and Thermal Ionization Mass Spectrometry for Analysis of Uranium and Plutonium Isotope Ratios, Federation of Analytical Chemistry and Spectroscopy Societies, Annual Meeting, Memphis, Tennessee, 2007.
[162] R.N. Taylor, T. Warneke, J.A. Milton, I.W. Croudace, P.E. Warwick, R.W. Nesbitt, Journal of Analytical Atomic Spectrometry 18 (2003) 480–484.
[163] J.E. Snow, J.M. Friedrich, International Journal of Mass Spectrometry 242 (2005) 211–215.
[164] L. Font, G.M. Nowell, D.G. Pearson, C.J. Ottley, S.G. Willis, Journal of Analytical Atomic Spectrometry 22 (2007) 513–522.
[165] S. Wakaki, S.-N. Shibata, T. Tanaka, International Journal of Mass Spectrometry 264 (2007) 157–163.
[166] X.L. Zhao, M.J. Nadeau, L.R. Kilius, A.E. Litherland, Nuclear Instruments and Methods in Physics Research B 92 (1994) 249–253.
[167] D.J. Rokop, D.N. Metta, C.M. Stevens, International Journal of Mass Spectrometry and Ion Physics 8 (1972) 259–264.
[168] IAEA, International Atomics Energy Agency, Nuclear forensics support–Reference manual, IAEA Nuclear Security Series No. 2, 2006, ISSN 1816-9317.
[169] WNIH, World Nuclear Industry Handbook, Nuclear Engineering International, 2005.
[170] R.W. Perkins, C.W. Thomas, Worldwide fallout, in: Hansen, al. et (Eds.), Transuranic Elements in the Environment, DOE/TIC-22800, Department of Energy, Washington, DC, 1980.
[171] IAEA, International Atomics Energy Agency, Safe Handling and Storage of Plutonium, Safety Reports Series No. 9, STI/PUB/1061, 1998, ISSN 1020-6450.
[172] A.S. Krivokhatsky, Yu.V. Dubasov, E.A. Smirnova, N.V. Skovorodkin, V.G. Savonenkov, B.M. Alexandrov, E.L. Lebedev, Journal of Radioanalytical and Nuclear Chemistry 147 (1991) 141–151.
[173] P. Peuser et al., Detection Methods for Trace Amounts of Plutonium, IAEA-SM-252/40, 1981.
[174] D. Arnold, Applied Radiation and Isotopes 64 (2006) 1137–1140.
[175] P. Hoffmann, K.K. Lieser, Methoden der Kern- und Radiochemie, VCH Verlagsgesellschaft mbH, 1991.
[176] K. Eberhardt, A. Kronenberg, Kerntechnik 65 (2000) 269–274.
[177] V.P. Perelygin, Y.T. Chuburkov, Radiation Measurement 28 (1997) 385–392.
[178] R. Jakopič, S. Richter, H. Kühn, L. Benedik, B. Pihlar, Y. Aregbe, International Journal of Mass Spectrometry 279 (2009) 87–92.
[179] J. Riegel, R. Deißenberger, G. Herrmann, S. Köhler, P. Sattelberger, N. Trautmann, H. Wendeler, F. Ames, H.J. Kluge, F. Scheerer, F.J. Urban, Applied Physics B 56 (1993) 275–280.
[180] R.L. Edwards, J.H. Chen, G.J. Wasserburg, Earth and Planetary Science Letters 81 (1986/1987) 175–192.
[181] S.J. Goldstein, M.T. Murrell, D.R. Janecky, Earth and Planetary Science Letters 96 (1989) 134–146.
[182] J.H. Chen, G.J. Wasserburg, Analytical Chemistry 53 (1981) 2060–2067.
[183] J.A. McLean, J.S. Becker, S.F. Boulyga, H.J. Dietze, A. Montaser, International Journal of Mass Spectrometry 208 (2001) 193–204.
[184] S.F. Boulyga, K.G. Heumann, Journal of Environmental Radioactivity 88 (2006) 1–10.
[185] L. Wacker, E. Chamizo, L.K. Fifield, M. Stocker, M. Suter, H.A. Synal, Nuclear Instruments and Methods in Physics Research B 240 (2005) 452–457.
[186] D. Tuttas, J.B. Schwieters, High Precision Strontium and Neodymium Isotope Analyses, Thermo Electron Corporation, 2003, Application Note: AN310015_E.